Light-cone representation of the quark Schwinger-Dyson equation

L. S. Kisslinger and O. Linsuain
Department of Physics, Carnegie Mellon University, Pittsburgh, Pennsylvania 15213
(Received 9 October 2001; published 29 October 2002)

We use a light-cone approach to solve the Schwinger-Dyson equation for the quark propagator in Minkowski space. We show how this method can be used to solve the equation beyond the spacelike region, to which one is usually restricted with the Euclidean-space approach. We work in the Landau gauge, use an infrared-enhanced model for the gluon propagator, and include instanton effects to get both confinement and vacuum condensates. With our models reasonable fits to known quantities are obtained, resulting in a light-cone quark propagator that can be used for hadronic physics at all momentum transfers.

DOI: 10.1103/PhysRevC.66.045206 PACS number(s): 12.38.Lg, 12.38.Aw, 14.65.Bt

I. INTRODUCTION

For a microscopic QCD description of hadrons and hadronic matter one needs the fully dressed nonperturbative quark and gluon propagators, for which the Schwinger-Dyson formalism is a natural approach. A full study of QCD, however, requires investigation of hadronic properties at all momentum transfers. Since an instant form of field theory is difficult to use for composite states at medium or high momentum, a light-cone representation is desirable [1]. In the present paper we develop a light-cone formulation of the Schwinger-Dyson equation for the quark propagator for use in developing hadronic light-cone Bethe-Salpeter amplitudes as well as providing new aspects of the quark propagator, which we discuss below.

The Schwinger-Dyson equations (SDE's) of a field theory embody all its dynamics (see Ref. [2] p. 475). They are the complete equations of motion for the Green's functions of the theory, and thus provide a natural way for studying the theory beyond the limited scope of perturbative expansions. Unfortunately they consist of an infinite tower of coupled integral equations relating full n-point functions to full $(n+1)$-point functions. Thus, the integral equation satisfied by one propagator may involve another propagator and a three-point vertex. The equation for this vertex may in turn include another propagator and a four-point vertex or scattering kernel, and so on. Some physically motivated truncation scheme becomes mandatory before the infinite tower can be brought to a manageable size. As has been stressed in Ref. [3] the Ward identities of gauge theories significantly ease this truncation, since they imply that two-point functions (propagators) uniquely determine the longitudinal part of three-point functions (vertices).

The SDE's for the fermion and gauge boson propagators in QCD and QED have been studied using different approximations and models. For an excellent review see Ref. [4], and references therein. A recurring topic in this area is the question of the analytic structure of the propagators. For the electron propagator one expects a singularity at $p^2=m_{phys}^2$. For a confined particle such as the quark it is not so clear what one should expect; it depends on what the confining mechanism is. Coleman (see Ref. [5] pp. 378–386) has shown that it is perfectly possible for a confined particle to have a pole in its propagator at a positive real (i.e., physical and timelike) value of p^2.

Fermion propagators with branch points at complex conjugate locations off the real axis of the variable p^2 have been obtained more than twenty years ago for QED [6], and more recently for QCD as well [4]. This has been studied in great detail by Maris [7]. In the case of QED, where we know that there must be a singularity at $p^2=m_{phys}^2$, this is thought to be an artifact of the approximations with no physical significance. For QCD, the absence of singularities on the real axis has been thought to be related to quark confinement. Şavkli [8] and Şavkli and Tabakin [8,9] have shown that the imaginary part of the value of p^2 where the singularity occurs may be interpreted as a decay width for a single quark state, and can be related to the hadronization distance, with reasonable results. However, the fact that in two physical situations as different as those of QED and QCD the singularities seem to have the same origin [7] makes any physical interpretation difficult. The location of these singularities poses yet another difficulty: it invalidates the Wick rotation, and thus makes the theory as defined in Euclidean metric not equivalent to that defined in Minkowski metric.

In this paper we study the SDE for the quark propagator starting from its Minkowski-space formulation. In solving the equation, we make assumptions about the location of the singularities similar to those necessary to justify a Wick rotation. However, our approach allows us to study the quark propagator for timelike as well as spacelike values of the momentum.

Our treatment of the SDE in a light-cone representation is discussed in detail in Sec. II. The method is an extension of the method used in perturbation theory [10] to obtain an infinite-momentum-frame formulation, which in many respects is equivalent to the light-cone field theory formulation of perturbative diagrams. It is also analogous to the method for obtaining a light-cone representation of the Bethe-Salpeter equation (BSE) from the standard four-dimensional instant form, however, as explained in Sec. II, the simple prescription for projecting onto the light cone cannot in general be used for the SDE.

In Sec. III we discuss our models. Section IV contains some technical aspects of solving the equations and test calculations in Minkowski space, using equations derived in the

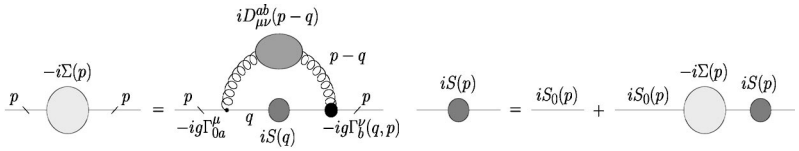

FIG. 1. Diagrammatic representation of the SDE for the quark propagator.

$$-i\Sigma(p)=\frac{g^2}{\omega^{d-4}}\int\frac{d^dq}{(2\pi)^d}(-i\Gamma^{\mu}_{0a})iS(q)(-i\Gamma^{\nu}_{b}(q,p))iD^{ab}_{\mu\nu}(p-q) \qquad iS(p)=iS_0(p)+iS_0(p)(-i\Sigma(p))iS(p)$$

Appendix. In Sec. V we present the results of our model calculations and in Sec. VI we give our conclusions.

II. THE QUARK SDE AND THE LIGHT CONE

In this section we discuss our light-cone formulation of the SDE. Since the light-cone representation of the BSE for bound systems is described extensively in the literature, we also briefly review the BSE, which provides motivation for the present work, and explain its applicability.

The full dressed quark propagator, $S(p)$, satisfies in d space-time dimensions the SDE (see Fig. 1):

$$S^{-1}(p)=S_0^{-1}(p)-\Sigma(p),$$

$$\Sigma(p)=\frac{ig^2}{\omega^{d-4}}\int\frac{d^dq}{(2\pi)^d}\Gamma^{\mu}_{0a}S(q)\Gamma^{\nu}_{b}(q,p)D^{ab}_{\mu\nu}(p-q), \tag{1}$$

where $\Gamma^{\nu}_{b}(q,p)$ and $D^{ab}_{\mu\nu}(p-q)$ are the dressed quark-gluon vertex and dressed gluon propagator, respectively. $\Sigma(p)$ is called the self-energy. Indices in Greek letters represent Lorentz indices and those in Latin letters stand for color indices. The quantity ω is the energy scale necessary in dimensional renormalization. The reason for working in dimension d in this paper is twofold. On one hand, we want to keep the approach general so that models with ultraviolet divergencies can be explored, and on the other hand, we present a sample calculation in Sec. IV of how such a divergence could be renormalized in the $\overline{\text{MS}}$ scheme numerically. This could be used to tackle the important question of whether or not dimensional renormalization can produce sensible physical results in a nonperturbative calculation. We do not try to answer that question in this paper. All our solutions to the SDE are obtained in models with no ultraviolet divergencies.

The color structure of all quantities in Eqs. (1) is known: The bare vertex is $\Gamma^{\mu}_{0a}=\gamma^{\mu}\lambda_a/2$, the dressed vertex is $\Gamma^{\nu}_{b}(q,p)=\Gamma^{\nu}(q,p)\lambda_b/2$, and the gluon propagator is $D^{ab}_{\mu\nu}(k)=\delta^{ab}D_{\mu\nu}(k)$, so that the color indices can be contracted: $\lambda_a\lambda_b\delta^{ab}=16/3$. The inverse bare propagator is $S_0^{-1}(p)=\not{p}-m_c$, with the current quark mass m_c being zero in the chiral limit or estimated from partially conserved axial-vector currents.

The solutions of the SDE are of the form

$$S^{-1}(p)=\not{p}A(p^2)-B(p^2). \tag{2}$$

Physically, the most significant aspect of the solution for the two functions $A(p^2)$ and $B(p^2)$ is the ratio $M(p^2)=B(p^2)/A(p^2)$, which is interpreted as the effective mass of quark. Since isolated quarks are confined, the interpretation of this mass is not as straightforward as for the electron SDE.

The light-cone formulation of quantum mechanics [1] starts with the demonstration that in the light-cone representation one obtains light-cone Poincaré generators, with an interaction-free Lorentz boost in one direction. One can also show that the analogous result is true in a light-cone field theory. This enables one to study high momentum transfer processes, such as form factors in the region above 1 GeV, which is very difficult in the instant form.

Before discussing the light-cone representation of the SDE we review the well-known light-cone representation of the BSE. Since in physical applications of the BS amplitudes to form factors and transition amplitudes one needs the dressed quark propagator, the main motivation for our present work is to formulate a light-cone Schwinger-Dyson equation to be used with the light-cone Bethe-Salpeter formalism in Minkowski space.

There has been a great deal of work on bound-state problems in light-cone representations based on the BSE. For example, the BSE for the pion in relative coordinates has the form

$$\Psi(k)=\int d^4l\mathcal{K}(k,l)\Psi(l), \tag{3}$$

where $\mathcal{K}$ is the kernel and Ψ is the BS amplitude. One can obtain a light-cone representation [11] by inserting a delta function to include the light-cone on-shell condition and eliminate the l^- variable,

$$\Psi(x,\mathbf{k}_\perp)=\int[dy][d^2\mathbf{l}_\perp]\mathcal{K}(x,\mathbf{k}_\perp;y,\mathbf{l}_\perp)\Psi(y,\mathbf{l}_\perp). \tag{4}$$

BS amplitudes from this type of equation have been used to study the transition from nonperturbative to perturbative regions [12,13]. We emphasize that for such calculations both on-shell and off-shell aspects of the functions $A(p^2)$ and $B(p^2)$ are needed. Therefore the prescription of projecting onto the light cone as for the BSE is not appropriate. We now discuss our approach to the SDE for the quark propagator on the light cone.

We solve Eq. (1) in a light-cone representation by using a method introduced originally for perturbation theory. In Ref. [10] Chang and Ma showed how the rules of light-cone perturbation theory[1] (LCPT) can be derived from the usual co-

[1]More accurately, their work refers to the Feynman rules in the infinite momentum frame, but the difference is of no bearing on our present discussion.

variant Feynman rules simply by changing into light-cone variables:

$$q^{\pm}=q^0\pm q^3, \quad \mathbf{q}_\perp=(q^1,q^2).$$

In simple calculations, such as a one-loop self-energy diagram of an electron in QED (or even of a quark in QCD), an important feature of the new rules becomes apparent: the range of integration over the q^+ variable becomes finite:

$$\int_{-\infty}^{+\infty} dq^+ \to \int_0^{p^+} dq^+,$$

where p^+ is the ''plus'' (longitudinal) component of the external momentum. As shown in Ref. [10], this feature is related to the fact that in LCPT there are no diagrams with lines going backwards in time and no vacuum diagrams (with the exception of zero modes and instantaneous terms in fermion propagators). This is a crucial property of light-cone field theory, since it simplifies tremendously the structure of the vacuum.

Consider now the form of the integrals needed for the calculation of the quark self-energy Σ in the SDE. In this case we are faced with the nonperturbative self-energy diagram seen in Fig. 1. Incidentaly, this diagram is analogous to its perturbative one-loop counterpart. The difference lies in the functional forms of the Green's functions involved. Without loss of generality, the integrals occuring in our SDE diagram can be written as a sum of terms of the form

$$\int \frac{d^dq}{(2\pi)^d} q^{\mu_1}q^{\mu_2}\ldots q^{\mu_n} f_Q(q^2+i\epsilon) f_G[(p-q)^2+i\epsilon], \tag{5}$$

where the f_Q contains factors coming from the quark propagator and possibly from the dressed vertex function, f_G contains factors coming from the gluon propagator and also possibly from the dressed vertex function, and the factors of q^{μ_i} come from factors ubiquitous of $\not{q}$. Since the external momentum p is held fixed during this integration, possible factors of p^{μ_i} and possible dependence of the Green's functions on p^2 are not relevant to the analysis below. In the present discussion we do not need the detailed form of our models, described in Sec. III, but only the aspects that give the singularities which must be considered in carrying out the integrals.

Consider first the scalar case, $n=0$ in Eq. (5), i.e., no factors q^μ. Using the variables

$$\alpha=q^+/p^+, \quad s'=q\cdot q, \quad s=p\cdot p, \quad \mathbf{q}'_\perp=\mathbf{q}_\perp-\alpha\mathbf{p}_\perp,$$

the integral in Eq. (5) becomes

$$\int \frac{ds'\,d\alpha\,d^{d-2}\mathbf{q}'_\perp}{2|\alpha|(2\pi)^d} f_Q(s'+i\epsilon) f_G[-\alpha^{-1}\mathcal{P}(q'^2_\perp,s,s',\alpha,\epsilon)], \tag{6}$$

where all the integrals are over the entire real line, and

$$\mathcal{P}(q'^2_\perp,s,s',\alpha,\epsilon)\equiv q'^2_\perp+\alpha(1-\alpha)(-s)+(1-\alpha)s'-i\alpha\epsilon$$

is reminiscent of the similar quantity that appears in the one-loop calculation after the well-known Feynman trick of combining denominators. Particularly, consider the case $f_G(s)=1/(s-m_1^2)^{a_1}$. The contribution to this integral coming from a simple pole in f_Q at $s'=m_0^2-i\epsilon$ becomes, after the $\mathbf{q}'_\perp$-integration,

$$\alpha^{-1}f_G(-\alpha^{-1}\mathcal{P}) \to \frac{(-1)^{-a_1}\alpha^{a_1-1}}{[\alpha(1-\alpha)(-s)+(1-\alpha)m_0^2+\alpha m_1^2-i\epsilon]^b},$$

where b is related to d, a_1, and to the strength of the singularity in f_Q. This is exactly what one gets when following Feynman's procedure for calculating the one-loop version of this integral, here with the longitudinal momentum fraction playing the role of the Feynman parameter. While this parallel between our light-cone approach to a nonperturbative calculation and the standard approach to a perturbative calculation cannot be taken too far (certainly we want to compute a nonperturbative quark propagator and do not want to model it with a perturbative one), we will make use of it in this paper to present a test of our numerical procedure. This is done in Sec. IV.

Returning to Eq. (6), let z_Q and z_G now be singular points of f_Q and f_G, respectively. Then the integrand in Eq. (6) has singularities in s' at points s'_1 and s'_2 whose imaginary parts are given by

$$\mathrm{Im}(s'_1)=\mathrm{Im}(z_Q)-\epsilon, \quad \text{and} \quad \mathrm{Im}(s'_2)=\frac{\alpha}{\alpha-1}[\mathrm{Im}(z_G)-\epsilon].$$

It is then clear that if we assume that both z_Q and z_G are on or below the real axis, then the corresponding singularities of the integrands s'_1 and s'_2 will be on opposite sides of the real axis if and only if $\alpha/(\alpha-1)<0$, i.e., $0<\alpha<1$. For values of α outside this interval, both singularities fall on the same side of the real axis, and the contour of the s' integration can be closed with a semicircle that does not contain either of them. Thus *if all the singularities of the functions f_Q and f_G occur on or below the real axis, only the interval* (0,1) *in the integration over α contributes to the integral*.[2] This reasoning is only a slight modification of the one presented in Ref. [10]. The integral in Eq. (6) then becomes

$$\frac{1}{4\pi}\int_{-\infty}^{+\infty}\frac{ds'}{2\pi}\int_0^1 d\alpha \int \frac{d^{d-2}\mathbf{q}'_\perp}{(2\pi)^{d-2}}\alpha^{-1} f_Q(s'+i\epsilon) f_G \times[-\alpha^{-1}\mathcal{P}(q'^2_\perp,s,s',\alpha,\epsilon)]. \tag{7}$$

We see that to preserve important features of light-cone theory (here reflected in the integral over α being over a finite range) we must make assumptions *a priori* about the location of the singularities in f_Q and f_G. Our assumptions

[2]We are tacitly assuming that the integrals are ultravioletly convergent and thus closing the contour with a semicircle at infinity introduces no additional contribution.

are much like the ones necessary to justify a Wick rotation. Our approach, however, allows us to solve the quark SDE for timelike values of the momentum p, a possibility not readily available after a Wick rotation.

The steps taken above to show that the integration over α is limited to the interval (0,1) are relevant in more than the formal sense of showing agreement with other light-cone calculations. In a numerical procedure, after the limit $\epsilon \rightarrow 0^+$ is taken, the exact locations of the singularities might get blurred. Considerations of what regions contribute must be made beforehand. A numerical integration over α over the entire real line would yield incorrect results. In Sec. IV we show through a numerical test that our form yields correct results.

The Green's functions involved in computing the self-energy in Eqs. (1) contain factors of $\not{q}$ and $\not{p}$. These lead to computing the integral in Eq. (5) with one or more factors q^{μ_i}.[3] As discussed in Ref. [10], in some cases the previous reasoning fails for some components of the integrals (usually referred to as ''bad'' components). The issue then arises as to whether or not one can avoid all such components. In all such cases we are able to avoid them and compute only the ''good'' components. The ''bad'' components are recovered by the requirements of Lorentz symmetry. The results for the integrals we need are given in the Appendix.

A comment on expression (7) as compared to a typical light-cone calculation is in order. In most light-cone calculations, the integral over all values of q^- [equivalent to the integral over all values of s' in Eq. (7)] is absent. An on-shell condition that determines the value of q^- is used instead. In other words, the calculations are performed in the light-cone version of the so-called old-fashioned time-ordered perturbation theory (TOPT). This has become so customary that the rules of light-cone TOPT are at times identified with the rules of light-cone theory.

The equivalence between TOPT (either light cone or equal time) and the Feynman rules is usually shown by closing a contour of integration to pick up a singularity in a propagator and thus put a particle on shell. This can be done in the equal-time formulation (by first doing the integral over q^0, for example) or in the light-cone formulation (by first doing the integral over q^-, for example). One should refrain from carrying out this procedure in the SDE, in either formulation. Most certainly, the singularities of the Green's functions involved are more complicated than just a simple pole. In this respect both the light-cone and the equal-time formulations are similar.

There is an important difference, however, in what a reader of this work *might expect to see*. While it has become the norm to see covariant four-dimensional Feynman rules when working in the equal-time formulation, it might have been expected that, in this paper, the light-cone approach would have gotten rid of one integration already in Eq. (7) by replacing it with an on-shell condition. Hopefully this comment clarifies why that is not so.

III. MODELS

There has been an extensive program of research on the SDE during the past decade. See Refs. [4,14] for reviews. The usual approach is to model the gluon propagator and to use symmetries to express the dressed vertex in terms of the propagators, or to use the free vertex. The model is constrained by the vacuum condensates. We follow this general procedure in our light-cone approach. Since our approach allows one to define meson form factors for all momentum transfers, which is not true of instant-form approaches, applications of our solutions to hadronic properties will be most interesting.

Since in all recent SDE calculations of the quark propagator either the bare vertex is used (the so-called Rainbow approximation) or identities are used to express the dressed vertex in terms of the dressed propagator (as we discuss in Sec. III B below), the main problem in obtaining a quark SDE that represents QCD is to find a realistic model for the gluon propagator. Recognizing that instantons can give the main nonperturbative QCD (NPQCD) physics in the midrange region, but do not give confinement, we employ two models: the polynomial model to give the infrared-enhancement aspects of QCD, and the instanton model for midrange NPQCD. An important part of our effort is to explore how one can use these two models simultaneously and minimize double counting. As we discuss in Sec. V, we are able to do this successfully.

The Lorentz tensor structure of the gluon propagator has the general form

$$D_{\mu\nu}(k)=\frac{-1}{k^2+i\epsilon}\left\{\left(g_{\mu\nu}-\frac{k_\mu k_\nu}{k^2+i\epsilon}\right)D(k^2)+\xi\frac{k_\mu k_\nu}{k^2+i\epsilon}\right\}. \tag{8}$$

Here ξ is the gauge parameter. The choice of a model is to pick a value of ξ, such as $\xi=0$ for the Landau gauge, to model the form of the function $D(k^2)$, and the vertex. The two essential nonperturbative features that the gluon propagator must be consistent with are confinement and the vacuum condensates. It has long been known that with the gluon propagator having a $1/k^4$ behavior there is confinement [15] and one can fit the string tension. On the other hand, it is also known that with the instanton liquid model [16] one can fit the quark and gluon condensates.

We explore two models for $D(k^2)$ in the present work. On one hand, we model the gluon propagator with a sum of terms, each containing a different power of the momentum. We refer to this as the polynomial model.[4] This allows for a tunable infrared enhancement of the gluon propagator. On the other hand we want to investigate the consequences of including instanton effects explicitly into the quark SDE (at

[3]For example, a factor of $\not{q}$ would imply looking at the integral with one factor q^μ (vector case), while a factor like $\not{q}\not{p}\not{q}$ would lead to an integral with a factor $q^\mu q^\nu$ (a second rank tensor), and so on.

[4]The name might not be the most appropriate: ''polynomial'' suggests a sum of terms involving variables to *integer* powers.

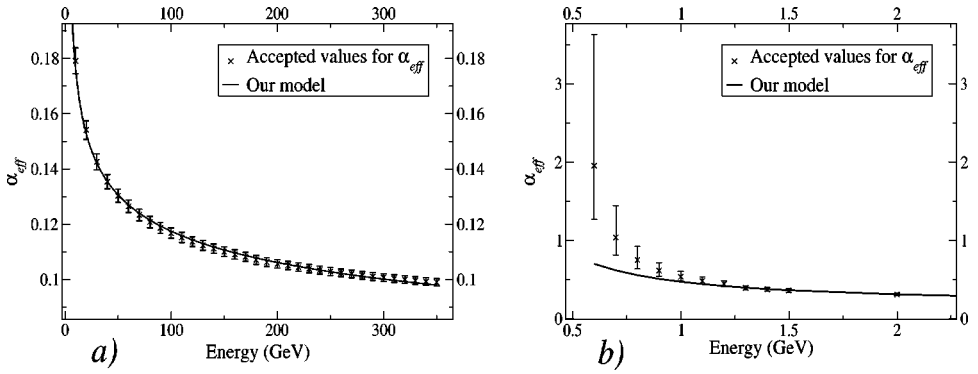

FIG. 2. Fitting α_{eff} with Eq. (11). See text for values of parameters. (a) For energies up to 350 GeV. (b) A closeup for lower energies.

the risk of double counting these effects). We refer to this as the instanton model. We discuss the double counting problem in Sec. V.

A. Polynomial model

We work in the Landau gauge with $\xi=0$, and take as our model gluon propagator

$$D_{\mu\nu}(k)=\frac{-1}{k^2+i\epsilon}\left(g_{\mu\nu}-\chi\frac{k_\mu k_\nu}{k^2+i\epsilon}\right)D(k^2), \tag{9}$$

with the parameter χ introduced to allow us to use a Feynman-like gauge [the gauge where $D_{\mu\nu}(k)\propto g_{\mu\nu}$]. Thus $\chi=0$ for the Feynman-like gauge and $\chi=1$ for the Landau gauge. See Refs. [4,14] for discussions the choice of gauge and gauge invariance for the SDE's in QCD.

It has been shown elsewhere [17] that renormalization group arguments yield an approximate relation between the renormalized coupling constant, the renormalized gluon propagator, and the effective coupling:

$$g_R^2 D_R(k^2)\approx g_{eff}^2(k^2)=4\pi\alpha_{eff}(k^2), \tag{10}$$

where the subscript R denotes renormalized quantities, and g_{eff} is the effective running coupling constant. The renormalized coupling is related to the running coupling by $g_R^2 \equiv g_{eff}^2(Q^2)|_{Q^2=\mu^2}$, where μ^2 is the renormalization point.

As discussed in Ref. [4] Sec. 6.1, Eq. (10), and the fact that in the Landau gauge only the combination $g^2D(k^2)$ enters the SDE, reduces the problem of modeling the nonperturbative part of the gluon propagator to that of modeling the nonperturbative part of α_{eff}. We model α_{eff} with the expression

$$\alpha_{eff}(k^2)=\sum_{l=1}^{N}(-1)^{c_l}\lambda_l\left(\frac{s_0}{k^2+i\epsilon}\right)^{c_l}. \tag{11}$$

Although the known logarithmic behavior of α_{eff} in the high energy limit cannot be fitted accurately with this form, a reasonable approximation can be obtained up to energies well beyond our main region of interest. Thus, for example, with $N=2$, $s_0=1$ GeV^2, $\lambda_1=0.222$, $c_1=0.07$, $\lambda_2=0.25$, and $c_2=0.6$ the values for α_{eff} obtained from our fit are within the accepted error bars as published, for example, by PDG[5] [18] for energies from about 1.3 GeV to 350 GeV (see Fig. 2). Fits to higher energies can always be achieved by adding more terms in Eq. (11) with smaller c_l. As can be seen in Fig. 2, with these parameters, our model underestimates the accepted values for α_{eff} in the important energy range of a few hundred MeV to about 1.2 GeV, although it is widely believed that it overestimates them in the deep infrared.

There is not complete certainty, however, about what happens to the effective coupling or to the gluon propagator at very low energies. Some results [19,17] suggest that the pole at $k^2=0$ gets enhanced and could be as strong as $1/k^4$. This would provide an explanation for confinement as shown by t'Hooft [15]. Other results from calculations within the Dyson-Schwinger formalism [20], and from lattice simulations [21], with confinement, suggest that the pole gets softer or disappears and that the gluon picks up an effective mass. Our model describes an infrared-enhanced gluon propagator, although not as strongly as $1/k^4$.

We now introduce the notation for the self-energy in the SDE, $\Sigma(p)$ in Eq. (1), for the polynomial model,

$$S^{-1}(p)=S_0^{-1}(p)-\Sigma_P(S), \tag{12}$$

where Σ_P is the SDE self-energy in the polynomial model, defined by Eqs. (9)–(11), and $S(p)$ is the dressed quark propagator in this model. Since the self-consistent calculation depends on $S(p)$, we include it as an argument of the self-energy $\Sigma_P(S)$. This notation is introduced since the solution for the quark propagator in the instanton medium that we discuss next was obtained in Ref. [22] from a similar self-consistent equation.

B. Instanton model

As we shall discuss in Sec. V below, one cannot obtain the known quark condensates with the polynomial model. On the other hand, it is known that with a pure instanton model one can obtain the quark condensate but not the string tension. For this reason we consider a model with quarks propa-

[5]Data for $\alpha_{\rm strong}$ taken from the PDG at http://www-theory.lbl.gov/~ianh/alpha/alpha.html

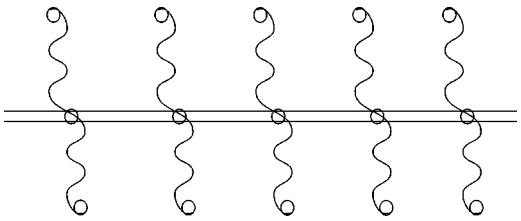

FIG. 3. Quark propagating in the instanton medium.

gating in the instanton medium and in addition the gluon propagator having a $1/k^{\alpha}$ structure to get infrared-enhancement effects.

Since the instanton forms have been obtained in Euclidean space, however, one must make an analytic continuation to obtain a Minkowski-space formulation, as was described in detail in the early days of using instantons for QCD bubble nucleation [5]. It has recently been shown that with a Minkowski-space form of an instanton piture with the purely gluonic Lagrangian for the bubble walls in the early universe QCD phase transition one obtains a reasonable estimate of the surface tension [23]. In the present work, however, where we employ a model for the quark propagator in the instanton background we do not explore the analytic continuation. This would be an important topic for a future investigation.

The starting point is the solution for the instanton using the classical action [24], which gives for the instanton color field

$$A^{inst}_{\mu(x)a}=\frac{2\eta_{a\mu\nu}x_{\nu}}{x^2+\rho^2}, \tag{13}$$

$$G^{inst}(x)\cdot G^{inst}(x)=\frac{192\rho^4}{(x^2+\rho^2)^4},$$

where ρ is the instanton size. The quark zero modes in the instanton background [25], for the + mode with the instanton at position z, are

$$\Psi_z(x)=\frac{\rho}{\sqrt{x^2}\pi(x^2+\rho^2)^{3/2}}\frac{1+\gamma_5}{2}\gamma_{\alpha}(x_{\alpha}-z_{\alpha})U, \tag{14}$$

where ρ is the instanton size and U is a unitary color-spin matrix. From this the widely used model of the quark propagating in the instanton–anti-instanton medium [28] was derived. In this model, the quark propagator $S_I(p)$ was calculated:

$$\begin{aligned} S_I(p)&=[\not{p}A_I(p^2)-B_I(p^2)]^{-1},\\ A_I(P)&=1,\\ B_I(P)&=KP^2f^2(\rho P/2),\\ f(z)&=\frac{2}{z}-[3I_0(z)+I_2(z)]K_1(z), \end{aligned} \tag{15}$$

where $K\approx 0.29\ \mathrm{GeV}^{-1}$, the instanton density $\rho\approx 1.667\ \mathrm{GeV}^{-1}$, $P=\sqrt{-p^2}$, and the I's and K_1 are modified Bessel functions of the first and second kind, respectively. The quark propagating in the instanton–anti-instanton medium is illustrated in Fig. 3.

In our instanton model we include instanton effects in the SDE by using the propagator in Eq. (15) to effectively add a contribution to the gluon propagator[6] that should account for the instanton effects. The exact forms used are discussed below. We are aware of the risk of double counting instanton effects with such a procedure. Being the complete equations of motion for the Green's functions of the theory, the SDE's should contain all nonperturbative effects, including those of instantons.[7] It is not clear, however, that the equation resulting after truncating the SDE and modeling the gluon propagator and the quark-gluon vertex still contains the instanton effects. That is exactly what we intend to explore, as well as the problem of double counting nonperturbative QCD effects.

Ultimately, the justification for this model is the scale separation of the different phenomena: the instantons give the nonperturbative QCD at the length scale of about 1/3 fm, while the polynomial model gives the far infrared behavior. As a simple example of the missing physics, if one uses only the polynomial model for the gluon propagator and ignores instanton effects consider a delta-function model for the gluon propagator. See, e.g., Ref. [14] for the solutions to the SDE in such a model. The quark and mixed quark condensates are given by

$$\langle 0|:\overline{q}(0)q(0):|0\rangle=-\frac{3}{4\pi^2}\int_0^{+\infty}dSS\frac{B(S)}{SA^2(S)+B^2(S)},$$

$$\begin{aligned} &\langle 0|:\overline{q}(0)g\sigma\cdot G(0)q(0):|0\rangle\\ &\quad=\frac{9}{4\pi^2}\int_0^{+\infty}dSS\left\{S\frac{B(S)[2-A(S)]}{SA^2(S)+B^2(S)}\right.\\ &\qquad\left.+\frac{81B(S)[2SA(S)\{A(S)-1\}+B^2(S)]}{16[SA^2(S)+B^2(S)]}\right\}. \end{aligned} \tag{16}$$

One can fit the strength of the delta-function gluon propagator to obtain the correct quark condensate. Then from Eqs. (16) it is simple to calculate the mixed quark condensate. The result is an order of magnitude different from the phenomenological value. This is an example of the need to include both the long-distance and the medium-distance nonperturbative QCD effects. We return to this when we discuss

[6]The contribution is explicitly added as an additional term in the SDE. Indirectly, it implies adding a correction to the gluon propagator.

[7]Instantons, however, open up the possibility of the presence of a so-called θ term in the QCD Lagrangian that is not considered when deriving the SDE's. Even so, all evidence suggests that such terms, if present at all, must be very small. See Ref. [26] Secs. 16.2 and 16.3, and references therein.

the results of our calculations. For completeness we include here the equation for f_π (see Ref. [4], Appendix C)

$$f_\pi^2=\frac{3}{4\pi^2}\int_0^{+\infty}dS\,\frac{SM(S)}{A(S)[S+M^2(S)]^2}\left[M(S)-\frac{S}{2}\frac{dM}{dS}\right].$$

Notice that in these equations P and S refer to Euclidean momenta.

We now discuss how we include instanton effects in the quark SDE. Although the solution given in Eqs. (15) for the propagator of a quark moving in an instanton background was obtained by the expansion of an integral equation [22] not derived from a Schwinger-Dyson formalism, it is possible and convenient for us to write that equation in a form analogous to that of a SDE, as in Eq. (12):

$$S_I^{-1}(p)=S_0^{-1}(p)-\Sigma_I(S_I), \tag{17}$$

where Σ_I is the kernel of an integral equation whose exact form is not necessary for the present argument,[8] and whose solution is the propagator S_I as given in Eqs. (15). Although this equation is not derived in Ref. [22] by modeling the gluon propagator in a SDE, we recognize that, in principle, it implies a model for the gluon propagator, namely, the model that would yield the solution given by Eqs. (15) in a true SDE. We use this observation in the following discussion.

Given that the self-energy is the *sum* of all one-particle-irreducible diagrams, one could think of writing an equation that would include both types of one-particle-irreducible diagrams as

$$S^{-1}(p)=S_0^{-1}(p)-[\Sigma_P(S)+\Sigma_I(S)], \tag{18}$$

where $\Sigma_I(S)$ is the self-energy with the gluon propagator which would give S_I in the SDE. Solving Eq. (17) for S_0^{-1} and substituting into Eq. (18) we immediately get

$$S^{-1}(p)=S_I^{-1}(p)-\Sigma_P(S)-[\Sigma_I(S)-\Sigma_I(S_I)]. \tag{19}$$

As a first approximation one could neglect the terms in the square brackets in this equation, and end up with

$$S^{-1}(p)=S_I^{-1}(p)-\Sigma_P(S). \tag{20}$$

Along a different line of thought, one could suggest that a term simply be added to the starting SDE to account for the contribution to the self-energy coming from the interaction of the propagator S_I with a cloud of gluons described by the polynomial model. This will result in an equation such as:

$$S^{-1}(p)=S_0^{-1}(p)-\Sigma_P(S)-\Sigma_P(S_I). \tag{21}$$

Finally we consider the case where besides adding this term, one proposes that it is the propagator S_I that should get dressed, i.e., that it is the quark moving through the instanton background (as opposed to just the free quark) that gets dressed with this gluonic cloud. That would result in

$$S^{-1}(p)=S_I^{-1}(p)-\Sigma_P(S)-\Sigma_P(S_I). \tag{22}$$

We discuss the results with Eqs. (12) and (20)–(22) and the question of double counting in Sec. V.

C. The vertex

The results reported in this paper were all obtained with the approximation $\Gamma_\mu(p,q)=\gamma_\mu$ (the so-called rainbow approximation). The popularity of this approximation is justified by its simplicity. It suffers the serious drawback of violating the Ward-Takahashi identity (WTI)

$$(p-q)^\mu\Gamma_\mu(p,q)=S^{-1}(p)-S^{-1}(q). \tag{23}$$

This identity holds in QED, and the forms for the vertex discussed below were proposed for QED. Such forms, however, are often used for QCD as well, since the analogous identity for QCD [known as the Slavnov-Taylor identity (STI)] (STI) reduces to Eq. (23) if ghost effects are ignored. Ignoring these effects is believed to be important in the infrared region.

This identity can be used to express the longitudinal part of the vertex in terms of the propagator. Ball and Chiu [22] have proposed the form

$$\Gamma_\mu(p,q)=\Gamma_\mu^{BC}(p,q)+\sum_{i-1}^{8}f^i(p^2,q^2,p\cdot q)T_\mu^i(p,q), \tag{24}$$

where the T_μ^i's are eight transverse tensors [i.e., tensors that satisfy $(p-q)^\mu T_\mu^i(p,q)=0$, and thus do not contribute to the WTI]. The form of these tensors is given in Eq. (3.4) of Ref. [27]. The eight scalar functions f^i are not constrained by the WTI. Γ_μ^{BC} is given by

$$\begin{aligned}\Gamma_\mu^{BC}(q,p)=&\gamma_\mu[A(q^2)(1-\beta_1)+A(p^2)\beta_1]\\&+(q+p)_\mu[\not{q}\beta_1+\not{p}(1-\beta_1)]\frac{A(q^2)-A(p^2)}{q^2-p^2}\\&-(q+p)_\mu\frac{B(q^2)-B(p^2)}{q^2-p^2}.\end{aligned} \tag{25}$$

This is really a small modification of the vertex proposed by Ball and Chiu. In their form $\beta_1=1/2$, but other values are often used to explore the effects of the transverse part. Besides compromising the symmetry of Γ_μ, changing the value of β_1 can have serious effects on renormalizability, because of its effect on the transverse part, as discussed below. The WTI itself is satisfied for any value of β_1, and for any choice of f^i's. The converse is also true: any vertex that satisfies the WTI can be expressed through Eqs. (24) and (25).

The vertex has been further constrained by other studies, in particular, Burden and Roberts [28] list a number of requirements Γ_μ should satisfy, besides the WTI. See also [4] Sec. 3.7. Exploiting these requirements, and particularly the

[8]One could, in principle, extract this form directly from either Eq. (7) or Eq. (12) of Ref. [22].

need to maintain multiplicative renormalizability in QED, Curtis and Pennington [29] narrowed down the last term in Eq. (24) to

$$\Gamma_\mu^{CP}(q,p)=\beta_2[\gamma_\mu(q^2-p^2)-(q+p)_\mu(\not{q}-\not{p})] \times\frac{(q^2+p^2)[A(q^2)-A(p^2)]}{(q^2-p^2)^2+[M^2(q^2)+M^2(p^2)]^2}. \quad (26)$$

Here too $\beta_2=1/2$ in the original formulation. Applying the approach explained in Sec. II, we have found that when using

$$\Gamma_\mu(q,p)=\Gamma_\mu^{BC}(q,p)+\Gamma_\mu^{CP}(q,p),$$

one must consistently set $\beta_1=\beta_2$. This ensures, for example, in a polynomial model with a term in Eq. (11) having $c_l=0$, that the function A remains free of divergencies in the Landau gauge, a well-established result. Notice that this implies that using just $\Gamma_\mu=\Gamma_\mu^{BC}$ is, in general, inconsistent.

We are currently investigating using this form in our model. Although that entails neglecting the effect of ghost fields in the STI, it is a significant improvement over the rainbow approximation. Also, He *et al.* have recently derived an identity similar to the WTI, but for the transverse fermion-gauge boson vertex [30], which we shall employ.

IV. THE NUMERICAL PROCEDURE

Equation (A6), derived in the Appendix using the approach described in Sec. II, is the basis for our numerical procedure for solving the quark SDE in Minkowski space. The light-cone approach used to obtain Eq. (A6), and in particular the treatment it makes of the singularities, contains some subtleties and technicalities. Here is a well-known example where using light-cone variables leads to a dead end[9]:

$$\lim_{\epsilon\to 0^+}\int\frac{dk_0dk_1}{(k_0^2-k_1^2-m_0^2+i\epsilon)^n}\quad n>1.$$

This integral is perfectly convergent and can be computed, for example, by closing the contour in the k_0 integration with a semicircle at infinity. The integral is, of course, nonvanishing. Using light-cone variables, one would get the integral

$$\lim_{\epsilon\to 0^+}\int\frac{dk^+dk^-}{2(k^+k^--m_0^2+i\epsilon)^n}\quad n>1.$$

If we now think of closing the contour of, say, the k^- integration, we see that the singularity occurs at $(m_0^2-i\epsilon)/k^+$. But then the singularity can always be avoided for any $k^+\neq 0$. Only for $k^+=0$ is the k^- integration nonvanishing, but then, it must have a delta-function-type singularity. In this example the shift in the location of the singularities due to the change to light-cone variables has transformed a simple situation into an intractable one.

[9]O.L. wishes to thank Matthias Burkardt for bringing this example to his attention.

The purpose of this section is to present a numerical test of Eq. (A6), as well as to point out some important technicalities. The idea is that with a "first guess" for the quark propagator in the form $S^{-1}(p)=\not{p}-m_0$, the output of the right-hand side of the SDE after the first iteration can be computed analytically using Eq. (A5), or numerically using Eq. (A6). Comparison of these two outputs provides information on the reliability of our procedure.

Once we verify that the procedure works accurately for just the first iteration, we can use it with confidence in further iterations. This is so because the accuracy of the procedure does not depend of the functional form used for $S(p)$ (the numerical procedure does not "know" that form).

As usual in numerical integration procedures, only the numerical values of the function $S(p)$ [or rather, of the functions $A(p^2)$ and $B(p^2)$] on a grid are used. The value of the integral is estimated by calculating the integral of a smooth function built over those numerical values, using a simple trapezoidal intrapolation or similar. The accuracy of the procedure then depends only on how well this smooth function approximates $S(p)$. This in turns depends on how smooth $S(p)$ is in the region in question, but not on its functional form. So, as long as the quark propagator does not develop singularities in the region being explored, the accuracy of the last (or any other) iteration in that region should be as good as that of the first. As already explained above, the only reason for using a simple perturbative quark propagator in this test is that for such a form of the propagator the value of the integral is well known analytically.

We then input the above described "first guess" for the quark propagator with $m_0=2$ GeV. Rather than using just one value for a_l in Eq. (A6), we use the full gluon propagator with parameters as described in Sec. III. Namely,

$$g_R^2D_R(k^2)=4\pi\left\{(-1)^{c_1}\lambda_1\left(\frac{s_0}{k^2+i\epsilon}\right)^{c_1} +(-1)^{c_2}\lambda_2\left(\frac{s_0}{k^2+i\epsilon}\right)^{c_2}\right\},$$

where $s_0=1$ GeV^2, $c_1=0.07$, $\lambda_1=0.222$, $c_2=0.6$, and $\lambda_2=0.25$ (here $a_l=1+c_l$). We will also discuss the ultraviolet divergent case $c_1=0$. For the vertex we set $\Gamma^\nu=\gamma^\nu$. With these forms we carry out the integrals in the SDE analytically using Eq. (A5) and numerically using Eq. (A6). We present graphs comparing the two outputs. We stress that these are not solutions to the SDE but merely the output of running the iterative procedure once. Solutions to the SDE are obtained using this same procedure repeatedly, but there one has no analytic result to check against. Those solutions are presented in Sec. V.

Keeping with tradition, the graphs are shown with a reversed x axis. We use the variable $S_E\equiv -s$, equivalent to the Euclidean invariant momentum squared. We show, however, negative values of S_E, which lay outside the usual Euclidean space, and represent the timelike region. The numerical integration is carried out up to $S_{E_{MAX}}=64$ GeV^2 and an estimate of the contribution of the remaining integration out to infinity

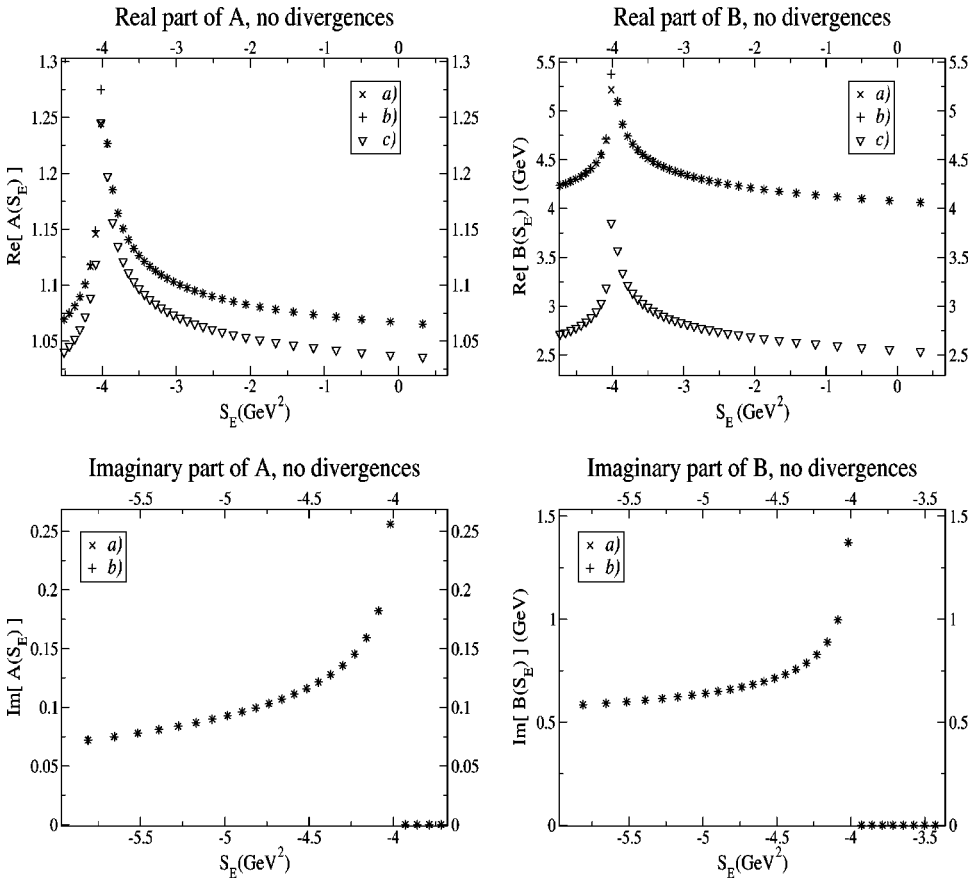

FIG. 4. Comparison of the numerical and analytic calculations of the quark propagator after one iteration. (a) Analytic result from Eq. (A5); numerical integrations of Eq. (A6): (b) with tail contribution, (c) without tail contribution. Notice the appearance of a singularity and an imaginary part.

("tail contribution") is added. As will be seen on the graphs the consequences of omitting this tail contribution are numerically important. In fact, in order to reproduce the numerical values of Eq. (A5), Eq. (A6) demands an elaborate integration procedure, which we now outline.

The integrand in Eq. (A6) is singular at $s'=s$, i.e., when the external and internal momenta are the same. We point out that this is a general feature of infrared-enhanced models, and not a consequence of our particular form for the gluon propagator. While this singularity never renders the integral divergent[10] in a formal sense, it does pose numerical difficulties, since one has to deal with sampling an unbounded integrand.

The computing market is full of numerical integration packages that handle all sorts of singularities, but one must be careful of what to use. The heart of the issue at hand can be grasped by examining Eq. (A6) carefully. It suffices to analyze the singularity occurring in the hypergeometric functions whose last argument is s'/s. When this argument is zero, these functions are perfectly regular (in fact, they equal one); when this argument is one, the functions are singular.

We then need to sample this function (and the whole integrand) at a fine grid between $s'/s=0$ and $s'/s=1$. But this is almost self-contradicting. When s is, say, the first point in the grid to the right of zero, what points are left for s' between zero and s? One needs a finer grid for s', of course. But this implies that we need the values of $f_Q(s')$ (from the previous iteration) on this finer grid. Eventually, it means that the computation *must start with a much finer grid than one on which one intends to obtain the final solutions*, at least in the deep infrared region. Since the behavior of the solutions in this region, and upon crossing over to the timelike region, is of great interest to us, we cannot allow for loss of accuracy there. The number of points in the initial grid would then have to grow exponentially with the number of iterations needed to solve the equation. The number of iterations could be anywhere from about a dozen (not small for exponential growth) to about a hundred.

One solution is to avoid model gluon propagators with infrared enhancement, e.g., to use a Gaussian model. We do not feel, however, that Gaussian models are appropriate in the timelike region, and one of the purposes of this paper is to explore the effects of a tunable infrared enhancement. We solve this problem as follows:

(i) Choose a reasonably fine grid in the region where the solutions are wanted.

(ii) Evaluate numerically just f_Q on that grid (the singularity we are considering now does not occur in f_Q).

(iii) Construct a simple intrapolating function on these values that approximates f_Q (using a trapezoidal method or similar).

(iv) The product of this simple intrapolating function times the rest of the integrand is then a good approximation to the integrand.

[10]The $i\epsilon$ procedure makes the contribution of this singularity well defined. An infrared divergence does appear in the integral over α in Eq. (A4), for $m_1=0$ and large a_l. In Eq. (A6) this divergence sits in the Γ functions.

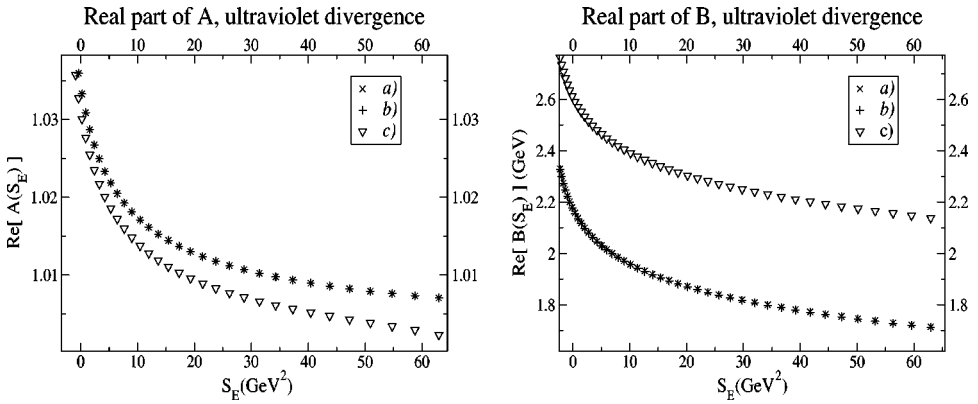

FIG. 5. Comparison of the numerical and analytical calculations of the $\overline{\text{MS}}$-renormalized quark propagator after one iteration in an ultraviolet divergent case. (a) Analytical subtraction in Eq. (A5); numerical integrations of Eq. (A6): (b) with tail contribution and $\overline{\text{MS}}$ subtraction, (c) without tail contribution or $\overline{\text{MS}}$ subtraction.

(v) Use the fact that this product can be integrated analytically to estimate the integral without further approximations.

This approach of sampling numerically only a part of the integrand in a numerical procedure is also used in the method of Gaussian quadratures. The rationale in that method is slightly different, however. A problem similar to the one we describe has been encountered in Ref. [7], as discussed there in Sec. 4.3.1.

Additionally, there is the ever present fact of having to integrate over all energies. Typically one integrates up to some large number. Once again this becomes a problem. One should integrate up to some value of s' large enough for the integrand to settle into its asymptotic behavior. In our case, this means values of s' large enough *as compared to s*, since for $s' \approx s$, the integrand is still displaying highly nontrivial behavior. Once again, how can this be done for the largest values of s? One needs a larger grid for s'. This now means that *the computation must start on a grid larger than one on which one intends to obtain the final solutions*. Furthermore, in Eq. (A5) the integrals are carried out to infinity. Divergencies, when they exist, are treated with the dimensional regularization method, not by integrating up to some cutoff momentum. In order to have Eq. (A5) as a reference, we choose to carry out the integrals in Eq. (A6) out to infinity as well. This is done as follows:

(i) From the last value of f_Q on the grid, and from its known or guessed behavior[11] for large momenta, construct a function to approximate f_Q at large s'.

(ii) The product of this function times the rest of the integrand is a good approximation to the integrand for large s'.

(iii) Use the fact that this product can be integrated analytically out to infinity to estimate the "tail contribution."

As the graphs below show, with this procedure the calculations become highly accurate, except around singularities in f_Q. Sure enough, extracting the behavior of the solutions around their own singularities is no easy task, but that represents a separate issue from the ones discussed here. In this work we do not attempt to extract that behavior. In Sec. V, we report the locations where the solutions seem to develop a singularity.

The graphs in Fig. 4 show the real and imaginary parts of the functions A and B after one iteration using the parameters above. As can be seen from the graphs, the procedure is quite accurate (provided the estimate of the tail contribution is added). The relative error is of the order of thousandths of a percent, although it is somewhat larger right before (but not after) the singularity at $S_E = -m_0^2$ (or $s = m_0^2$). As pointed out above this is not the singularity treated with the procedure discussed in detailed above. The contribution from this singularity was extracted by using the $i\epsilon$ procedure suggested by the argument of f_Q in Eq. (A4) and dropped in Eq. (A6). For values of s just larger than m_0^2 (or, in the graphs, values of S_E right before the singularity) there is not enough points to sample in order to extract the principal value accurately. For values of s just smaller than m_0^2 (or, in the graphs, values of S_E right after the singularity), the singularity occurs outside the integration region and does not affect the calculation [as seen in Eq. (A6), the integration into the timelike region stops at $s' = s$]. This is the reason why accuracy is affected only on one side of the singularity.

While this concerns a sample calculation with a bare propagator, a singularity in the dressed propagator will have similar consequences. In this sample calculation the fact that the exact location and nature of the singularity is already known has been exploited. This would not be as straightforward in further iterations. The imaginary parts shown in the graphs were obtained from the same $i\epsilon$ procedure.

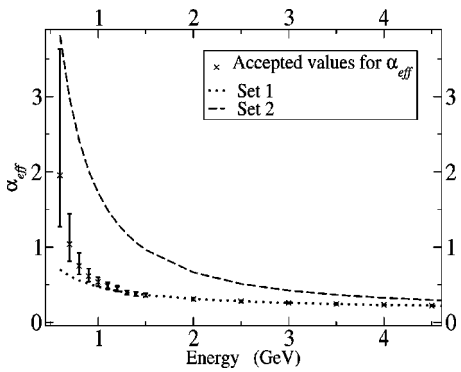

FIG. 6. Two different fits to α_{eff}.

[11]When the behavior was guessed, the correctness of such a guess was verified *a posteriori*. The calculation was repeated until agreement was reached in this sense.

TABLE I. Numerical results.

Model	Vertex: $\Gamma^\nu=\gamma^\nu$, rainbow approximation $(-\langle:\bar{q}q:\rangle)^{1/3}$ (MeV)		$(-\langle:\bar{q}g\sigma\cdot Gq:\rangle)^{1/5}$ (MeV)		f_π (MeV)		$M(0)$ (MeV)	
	Set 1	Set 2	Set 1	Set 2	Set 1	Set 2	Set 1	Set 2
Equation (27)	58	288.5	313.5	1111.5	13	89	86.5	770.5
Equation (28)	221	227.5	558	906.5	91.5	117.5	534	1084.5
Equation (29)	171.5	153.5	509	975.5	58.5	54.5	308	752.5
Equation (30)	219	159.5	624	1001	91	60	607	804
For comparison								
Equations (15)	216.7		456.5		86		417.6	
Other calculations	200–250		400–600		92		~300	
	Sum rules, lattice QCD				Experiment		NRQM [a]	

[a]See footnote 12.

Figure 5 shows the *renormalized* real parts of the same functions, with the crucial difference of setting $c_1=0$, rather than $c_1=0.07$. This causes an ultraviolet divergence. The imaginary parts in this calculation contain no divergence, so they remain basically the same as in the convergent case, and are not shown. In this case, the analytic results are renormalized in the $\overline{\text{MS}}$ scheme. The numerical calculation was performed with $d=4+2e$, where $e=-10^{-7}$. The divergence comes in the tail contribution (which is almost constant for the divergent term), and it is canceled by a numerical $1/e$ subtraction in the $\overline{\text{MS}}$ scheme. The well-known result that A is free of ultraviolet divergencies in the Landau gauge renders this function insensitive to whether or not the subtraction is performed. Addition of the tail contribution, however, still significantly affects the nondivergent term ($c_2=0.6$). For B, it is possible to obtain a finite result by just dropping the tail contribution (this would amount to cutoff renormalization), but integrating to infinity and performing the $1/e$

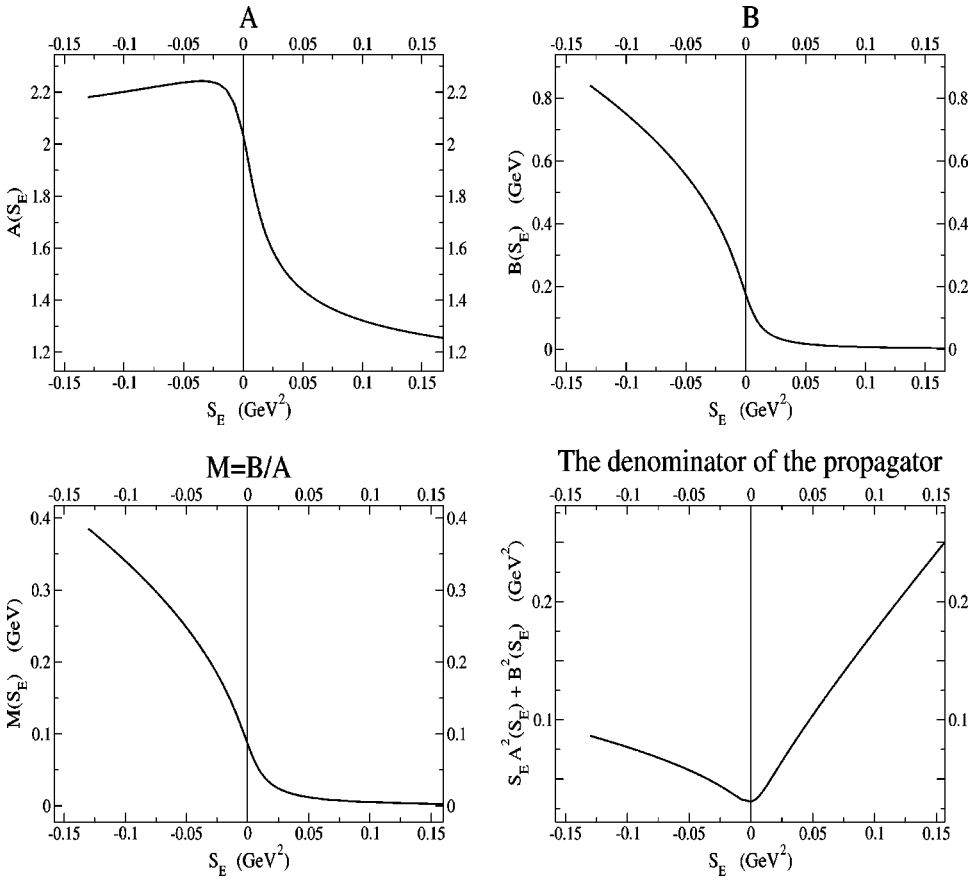

FIG. 7. Solutions to Eq. (27) using set 1. The left part of the graphs ($S_E<0$) represents the timelike region.

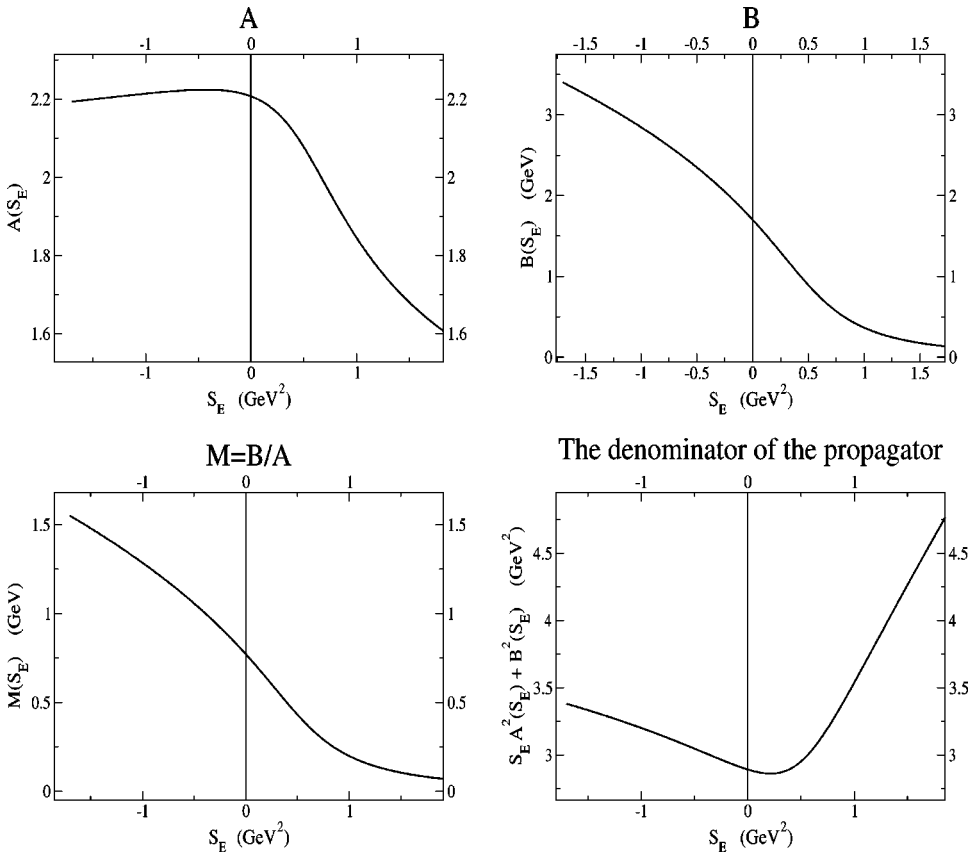

FIG. 8. Solutions to Eq. (27) using set 2. The left part of the graphs ($S_E<0$) represents the timelike region.

subtraction brings agreement with the renormalized result from Eq. (A5). We do not include in this paper solutions to the SDE involving this renormalization procedure, but thought it appropriate to show how such solutions could be obtained. We point out that it is not clear that dimensional renormalization yields physically correct results in nonperturbative calculations. This method could be used to explore that important question.

$$S^{-1}(p)=S_0^{-1}(p)-\Sigma_P(S), \tag{27}$$

$$S^{-1}(p)=S_I^{-1}(p)-\Sigma_P(S), \tag{28}$$

$$S^{-1}(p)=S_0^{-1}(p)-\Sigma_P(S)-\Sigma_P(S_I) \tag{29}$$

$$S^{-1}(p)=S_I^{-1}(p)-\Sigma_P(S)\Sigma_P(S_I), \tag{30}$$

V. RESULTS AND DISCUSSION

In the present section we give numerical results obtained in models that do not contain instanton contributions explicitly, and in models that do. As discussed at the end of Sec. III B, we study four different variants of the SDE, which we list here again for easy reference: as a reminder, Eq. (27) is just Eq. (1) with the polynomial model for the gluon propagator and does not explicitly include the instanton effects contained in Eqs. (15), while Eqs. (28)–(30) propose three different ways in which instanton effects could be included.

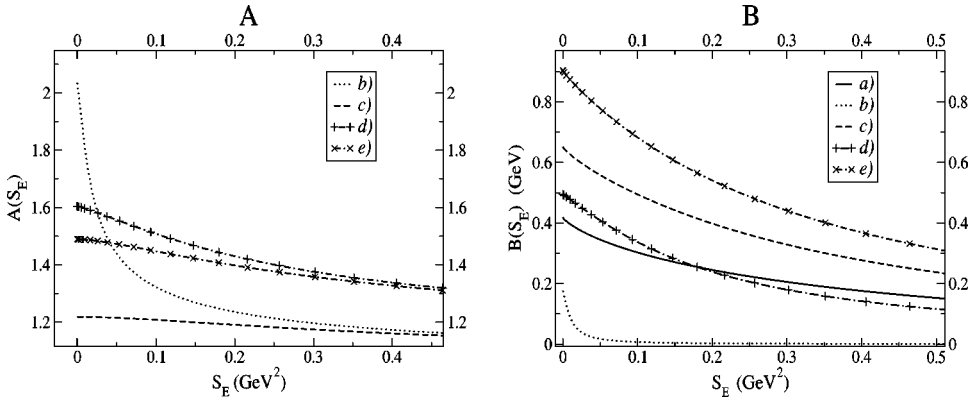

FIG. 9. Solutions to the SDE using set 1 in the spacelike region. (a) Result of Eqs. (15) from Ref. [22], (b) Eq. (27), (c) Eq. (28), (d) Eq. (29), and (e) Eq. (30). In (a) $A=1$, not shown.

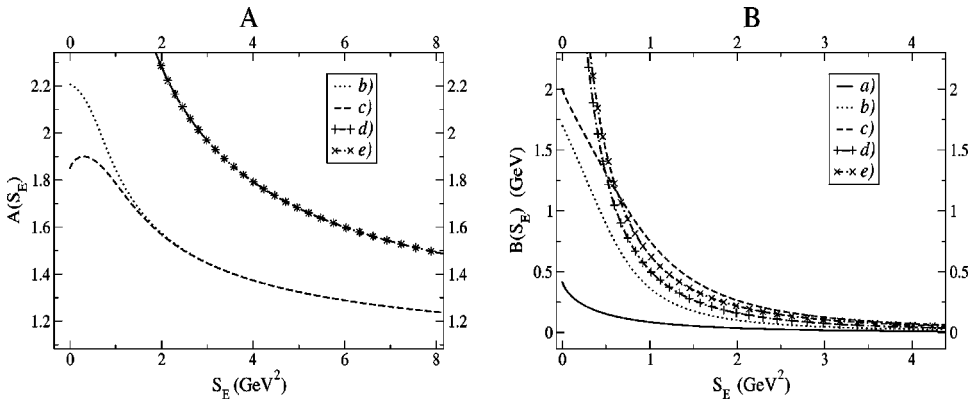

FIG. 10. Solutions to the SDE using set 2 in the spacelike region. (a) Result in Eqs. (15) from Ref. [22], (b) Eq. (27), and (c) Eq. (28), (d) Eq. (29), and (e) Eq. (30). In (a) $A=1$, not shown.

We use two different sets of parameters for the gluon propagator and the rainbow approximation for the vertex. All calculations were performed in the Landau gauge and in the chiral limit ($m_c=0$). The parameters for the gluon propagator are

$$\text{set 1:}\quad \begin{cases} \lambda_1=0.222, & c_1=0.07, \\ \lambda_2=0.25, & c_2=0.6, \end{cases}$$

$$\text{and set 2:}\quad \begin{cases} \lambda_1=0.222, & c_1=0.07, \\ \lambda_2=1.5, & c_2=0.85. \end{cases}$$

Parameter set 1 and the fit it generates to the coupling constant were already discussed in Sec. III A. Parameter set 2 is introduced in order to improve the poor fit to the phenomenological quantities (described below) obtained with parameter set 1 when the instanton contributions are not included [i.e., when solving Eq. (27)].

A comparison between both sets of parameters in terms of how well they fit α_{eff} is given in Fig. 6. It is clearly seen that parameter set 2, while producing a better fit to the phenomenological quantities, entails a much larger value for the coupling constant for energies under 5 GeV.

In Table I we give the values obtained for the quark condensate $\langle:\bar{q}q:\rangle$, the mixed quark condensate $\langle:\bar{q}g\sigma\cdot Gq:\rangle$, the pion decay constant f_π, and the value[12] of $M=B/A$ at $p^2=0$ from the solutions to all four equations with each parameter set.

Most of the results obtained from Eq. (27) (no instanton effects) with parameter set 1, appear too low. This is most likely due to the fact that with this parameter set the coupling constant is too weak in the crucial region of a few hundred MeV to about 1.2 GeV. Inclusion of the instanton effects seems to improve matters considerably, perhaps with the exception of Eq. (29). A plausible explanation for this may be as follows.

An important feature of Eq. (19), discussed in Sec. III B, to include instanton effects, is the presence of S_I^{-1} instead of S_0^{-1} in the inhomogeneous term, which occurs also in Eqs. (28) and (30), but not in Eq. (29). In fact, Eq. (28) can be regarded as an approximation to Eq. (30) up to terms of order $S(p)-S_I(p)$, which can be considered small, as opposed to $S_0^{-1}-S_I^{-1}$, which obviously is not small.

The results obtained from Eq. (27) (no instanton effects) with parameter set 2, appear closer to the correct values, often overestimating them. This is most likely due to the fact that parameter set 2 displays stronger infrared enhancement and overestimates the coupling the intermediate region (see Fig. 6). Inclusion of the instanton effects with parameter set 2, in most cases, does not lead to worse overestimation, as could be naively expected. With parameter set 1 we have a situation where the polynomial part of our model is contributing very little in the intermediate region (which we believe to be crucial to the quantities we are computing), and the instanton effects bring in the bulk of the contribution. With parameter set 2 both parts are contributing significantly, but their effects do not add up. Thinking along the lines of the approach implied by Eq. (18) and the discussion that follows, this probably means that the two types of contributions to the self-energy are of a different nature and they do not always interact constructively. This suggests that the instanton effects are *not* being double counted with this procedure, although such conjecture needs further testing.

Figures 7 and 8 show graphs of the solutions obtained using parameter sets 1 and 2, respectively, in Eq. (27). The focus is on the low energy spacelike region (right half of the graphs) and the crossover to the timelike region (left half of the graphs). Already at small timelike energies—the graphs show energies up to about 360 MeV for parameter set 1 and 1.3 GeV for parameter set 2—the behavior of the functions has changed dramatically from their behavior in the spacelike region. The function A, for example, stops growing, and, say, the function M for parameter set 1 (see Fig. 7), which barely rises from its asymptotic value of $M(p^2)\to m_c=0$ at large spacelike p^2 to about 90 MeV at $p^2=0$, soars up to almost 400 MeV already at $p^2\approx(360\ \text{MeV})^2$ (timelike).

[12]This value is often compared to the constituent quark mass (M_Q) of the nonrelativistic quark model (NRQM). As we show in Figs. 7 and 8, the solutions to the SDE vary quite rapidly upon entering the timelike region. The value M_Q should therefore, at best, be regarded as a rough guide to the value of B/A at $p^2=0$..

Of interest is also the behavior of the function $F(S_E) \equiv S_E A^2(S_E) + B^2(S_E)$, the denominator of the propagator. The vanishing of this function would indicate a pole in the quark propagator. Extrapolation of the behavior in the spacelike region would suggest a pole at much smaller timelike energies than those we have plotted, particularly for parameter set 1 (for set 2 some turning around is already noticeable at very low spacelike energies). The behavior of F right around its zero, if there is one, would be difficult to extract, since the functions A and B become singular there (see the discussion in Sec. IV).

F does seem to drop fast just to the left of the regions we have plotted. Thus, there seems to be a singularity in the quark propagator on the real axis, in our polynomial model. The singularity would be at $p^2 \approx (360\ \mathrm{MeV})^2$ for parameter set 1, and $p^2 \approx (1.3\ \mathrm{GeV})^2$ for parameter set 2. Further investigation of the solutions deeper into the timelike region is necessary before this can be ascertained. Notice that this refers to Eq. (27) only.

This fact is relevant to considerations on the validity of a Wick rotation. The presence of singularities in the quark propagator above the real axis creates difficulties with the Wick rotation. A prerequisitive to not having singularities above the real axis is to have them *on* the real axis,[13] since we know they must occur somewhere. Of course, many questions remain open. The exact location of this singularity, and the possibility of others, should be studied in this and other models. Nonetheless, we consider it a good indication that, in our model, the Euclidean and Minkowski approaches are probably equivalent.

Figures 9 and 10 compare the solutions to Eqs. (27)–(30) for parameters sets 1 and 2, respectively. For comparison, the solution given by Eqs. (15) obtained in Ref. [22] has been included as well. The figures include only the spacelike region (Euclidean space), since Eqs. (28)–(30) use the result in Eqs. (15) from Ref. [22], which was obtained in Euclidean space. The analytic continuation of this result into the timelike region exhibits a branch point at $p^2 = 0$ and thus has not been used.

VI. CONCLUSIONS

We have shown how to obtain a light-cone form of the SDE for the quark propagator. For QCD the key question is the infrared behavior of the gluon propagator, for which we have used two models. Knowing that the t'Hooft model [15] gives confinement, we have used polynomial models for the gluon propagator. Although the instanton liquid form [16] for the gluon propagator does not confine, and therefore does not have the correct far infrared behavior, it provides the main midrange QCD interaction, and allows fits to the condensates, which is essential for obtaining hadronic properties. With our approach we can obtain solutions for both the enhanced infrared behavior of the polynomial type models or the regular infrared behavior of the instanton model and recent lattice gauge calculations [28]. With the polynomial model we are able to work in Minkowski space and obtain solutions. With the models that include instanton effects we are able to obtain solutions that give much better agreement with the phenomenological values of the condensates.

We consider the present work exploratory. It provides the framework for obtaining light-cone QCD propagators that can be used to obtain light-cone models of hadronic BS amplitudes for studies of hadronic properties at all momentum transfers.

[13] Having the singularities below the real axis will not save the day, since that leads to singularities above the real axis.

ACKNOWLEDGMENTS

This work was supported in part by NSF Grant No. PHY-00070888. The authors would like to thank the P25 group at Los Alamos National Laboratory for hospitality when part of this work was done, and Andrew Harey and Montaga Aw for many helpful discussions. We would especially like to thank Pieter Maris for providing us with his Ph.D. thesis.

APPENDIX: INTEGRATING THE EQUATIONS

In this appendix results are given for integrals that we encounter when using our models for the SDE, described in Sec. III. In order to solve Eq. (1) in our model, we need to calculate integrals of the type [here $a_l = 1 + c_l$, with c_l as introduced in Eq. (11)]

$$\lim_{\epsilon \to 0^+} \int \frac{d^d q}{(2\pi)^d} \frac{f_Q(q^2 + i\epsilon)}{[(p-q)^2 - m_1^2 + i\epsilon]^{a_l}} \{1, q^\mu, q^\mu q^\nu\}$$
$$\equiv \{C_{00}(p^2; f_Q, a_l), p^\mu C_{10}(p^2; f_Q, a_l), p^\mu p^\nu C_{20}(p^2; f_Q, a_l) + g^{\mu\nu} C_{01}(p^2; f_Q, a_l)\}, \quad \text{(A1)}$$

where we include the cases with no factors, one factor, and two factors q^{μ_i}, and we exploit the Lorentz structure to define the scalar quantities C_{rj}.

These integrals include as a particular case the well-known integrals:

$$\lim_{\epsilon \to 0^+} \int \frac{d^d q}{(2\pi)^d} \frac{\{1, q^\mu, q^\mu q^\nu\}}{(q^2 - m_0^2 + i\epsilon)^{a_0} [(p-q)^2 - m_1^2 + i\epsilon]^{a_l}}$$
$$\equiv \{I_{00}(p^2; a_0, a_l), p^\mu I_{10}(p^2; a_0, a_l), p^\mu p^\nu I_{20}(p^2; a_0, a_l) + g^{\mu\nu} I_{01}(p^2; a_0, a_l)\}. \quad \text{(A2)}$$

This fact is useful because, for this particular case, the integrals are well known analytically. This is used in Sec. IV to present a numerical test of our integration procedures.

For $(r, j) = (0,0)$, (1,0), (2,0), and (0,1), the I's are known to be

$$I_{rj}(s;a_0,a_l)=\frac{i(-1)^{-(a_0+a_l)}(-1/2)^j}{(4\pi)^{d/2}}\Gamma\left[\begin{matrix}a_0+a_l-d/2-j\\ a_0,a_l\end{matrix}\right]$$

$$\times\int_0^1 d\alpha\frac{\alpha^{a_l+r-1}(1-\alpha)^{a_0-1}}{[\alpha(1-\alpha)(-s)+(1-\alpha)m_0^2+\alpha m_1^2-i\epsilon]^{a_0+a_l-d/2-j}},\tag{A3}$$

where we have used the compact notation

$$\Gamma\left[\begin{matrix}a_1,a_2,\ldots,a_n\\ b_1,b_2,\ldots,b_m\end{matrix}\right]=\frac{\Gamma(a_1)\Gamma(a_2)\ldots\Gamma(a_n)}{\Gamma(b_1)\Gamma(b_2)\ldots\Gamma(b_m)}.$$

For the C's, we proceed as explained in Sec. II, in particular as given in Eq. (7), to get

$$C_{rj}(s;f_Q,a_l)=\frac{i(-1)^{-a_l}(-1/2)^j}{(4\pi)^{d/2}}\Gamma\left[\begin{matrix}a_l+1-d/2-j\\ a_l\end{matrix}\right]\int_{-\infty}^{+\infty}\frac{f_Q(s'+i\epsilon)ds'}{2\pi i}$$

$$\times\int_0^1 d\alpha\frac{\alpha^{a_l+r-1}}{[\alpha(1-\alpha)(-s)+(1-\alpha)s'+\alpha(m_1^2-i\epsilon)]^{a_l+1-d/2-j}}.\tag{A4}$$

At this point we want to make sure that if we set $f_Q(s')=1/(s'-m_0^2)^{a_0}$, then Eq. (A4) agrees with Eq. (A3). This is most easily done by closing the contour of integration of the s' variable with an infinite semicircle in the *lower* half of the complex plane to pick up the singularity[14] in f_Q. While this becomes a rather simple exercise in contour integration, and agreement between the two forms is readily shown, this is not useful for our purposes. In this calculation one is using the analytic form of f_Q, which makes the approach not applicable to other forms of f_Q. We need a procedure that would rely only on the numerical values of f_Q. We perform the integrations by closing our contour with an infinite semicircle on the *upper* half of the complex plane to pick up the singularity (in s') of the expression on the second line of Eq. (A4). For $m_1=0$, the I's are known to be[15]:

$$I_{rj}(s;a_0,a_l)=\frac{i(-1)^{-(a_0+a_l)}(-1/2)^j}{(4\pi)^{d/2}(m_0^2)^{a_0+a_l-d/2-j}}$$

$$\times\Gamma\left[\begin{matrix}a_0+a_l-d/2-j,a_l+r,d/2+j-a_l\\ a_0,a_l,d/2+j+r\end{matrix}\right]{}_2F_1(a_0+a_l-d/2-j,a_l+r;d/2+j+r;s/m_0^2).\tag{A5}$$

For $m_1=0$, closing the contour in the lower half on the complex plane, we get for the C's

[14]If a_0 is not an integer, then this singularity will be a branch point with its corresponding branch cut, as opposed to a simple pole.
[15]The expansion of this expression about $d=4$ is probably more familiar to the expert in dimensional regularization.

$$C_{rj}(s;f_Q,a_l)=-\frac{i(-1)^{-a_l}(-1/2)^j}{(4\pi)^{d/2}\Gamma[a_l]}$$

$$\times\begin{cases}\Gamma\begin{bmatrix}b\\1+b-a\end{bmatrix}(-s)^{-b}\int_0^s ds' f_Q(s')(-s')^{b-a}{}_2F_1(1+b-c,b;1+b-a;s'/s)\\ +\Gamma\begin{bmatrix}b,c-b\\c,1-a\end{bmatrix}\int_s^{-\infty} ds' f_Q(s')(-s')^{-a}{}_2F_1(a,b;c;s/s') & s<0,\\ \Gamma\begin{bmatrix}b,c-b\\c,1-a\end{bmatrix}\int_0^{-\infty} ds' f_Q(s')(-s')^{-a} & s=0,\\ \Gamma\begin{bmatrix}c-b\\1+c-a-b\end{bmatrix}s^{1-c}\int_s^0 ds' f_Q(s')(s-s')^{c-a-b}(s')^{b-1}{}_2F_1(1-a,1-b;1+c-a-b;1-s/s')\\ +\Gamma\begin{bmatrix}b,c-b\\c,1-a\end{bmatrix}\int_0^{-\infty} ds' f_Q(s')(-s')^{-a}{}_2F_1(a,b;c;s/s') & s>0,\end{cases} \tag{A6}$$

where $a=a_l+1-d/2-j$, $b=a_l+r$, and $c=d/2+j+r$. Agreement between Eqs. (A5) and (A6) when $f_Q(s')=1/(s'-m_0^2)^{a_0}$ can now be shown by using a numerical procedure to perform the integrals in Eq. (A6). The procedure is outlined and a numerical test is presented in Sec. IV. Equation (A6) is the basis for all the numerical results obtained in this paper.

[1] P.M. Dirac, Rev. Mod. Phys. **21**, 392 (1949).
[2] C. Itzykson and J.B. Zuber, *Quantum Field Theory* (McGraw-Hill, New York, 1986).
[3] M. Baker, J.S. Ball, and F. Zachariasen, Nucl. Phys. **B186**, 531 (1981).
[4] C. Roberts and A.G. Williams, Prog. Part. Nucl. Phys. **33**, 447 (1994).
[5] S. Coleman, *Aspects of Symmetry* (Cambridge University, Cambridge, England, 1988).
[6] D. Atkinson and D.W.E. Blatt, Nucl. Phys. **B151**, 342 (1979).
[7] P. Maris, Ph.D. thesis, Institute for Theoretical Physics, 1993.
[8] Ç. Şavkli, Ph.D. thesis, University of Pittsburgh, 1997.
[9] Ç. Şavkli and F. Tabakin, Nucl. Phys. **A628**, 645 (1998).
[10] S. Chang and S. Ma, Phys. Rev. **180**, 1506 (1969).
[11] G.P. Lepage and S.J. Brodsky, Phys. Rev. D **22**, 2157 (1980).
[12] O.C. Jacob and L.S. Kisslinger, Phys. Rev. Lett. **56**, 225 (1986); Phys. Lett. B **243**, 323 (1990).
[13] L.S. Kisslinger and S.W. Wang, Nucl. Phys. **B399**, 63 (1993).
[14] P.C. Tandy, Prog. Part. Nucl. Phys. **39**, 117 (1997).
[15] G. t'Hooft, Nucl. Phys. **B75**, 461 (1974).
[16] T. Schaefer and E.V. Shuryak, Rev. Mod. Phys. **70**, 323 (1998).
[17] U. Bar-Gadda, Nucl. Phys. **B163**, 312 (1980).
[18] Particle Data Group, D. Groom *et al.*, Eur. Phys. J. C **15**, 1 (2000); URL http://pdg.lbl.gov
[19] N. Brown and M.R. Pennington, Phys. Rev. D **38**, 2266 (1988).
[20] A. Hauck, R. Alkofer, and L. von Smekal, hep-ph/9804387.
[21] F.D.R. Bonnet, P.O. Bowman, D. Leinweber, and A.G. Williams, hep-lat/0002020.
[22] P.V. Pobylitsa, Phys. Lett. B **226**, 387 (1989).
[23] L.S. Kisslinger, hep-ph/0202159.
[24] A.A. Belavin, A.M. Polyakov, A.S. Schwartz, and Yu.S. Tyupkin, Phys. Lett. **59B**, 85 (1975).
[25] G. t'Hooft, Phys. Rev. D **14**, 3432 (1976).
[26] T.-P. Cheng and L.-F. Li, *Gauge Theory of Elementary Particle* (Oxford University Press, New York, 1984).
[27] J.S. Ball and T.W. Chiu, Phys. Rev. D **22**, 2250 (1980).
[28] C.J. Burden and C.D. Roberts, Phys. Rev. D **47**, 5581 (1993).
[29] D.C. Curtis and M.R. Pennington, Phys. Rev. D **42**, 4165 (1990).
[30] H. He, F.C. Khanna, and Y. Takahashi, Phys. Lett. B **480**, 222 (2000).